Aerodynamics of Ice Remnants from Protected Surfaces

Andy P. Broeren* and Michael B. Bragg†
University of Illinois at Urbana-Champaign, Urbana, Illinois 61801

This paper presents a compilation of aerodynamic data for airfoils with ice remnants. Ice remnants is defined as ice accretion associated with the operation of ice-protection systems. Changes in drag and maximum lift coefficient are summarized for many different cases. It was found that there is a lack of data for residual ice simulations on airfoils, where the leading edge and stagnation region is free of ice roughness. In contrast, there are numerous studies detailing the aerodynamic effects of intercycle ice. In the case of spanwise-ridge ice resulting from heated leading-edge ice-protection systems (runback ice) or SLD accretions, there is also a lack of data for real ice accretion or high-fidelity simulations on airfoils. The existing data indicate that uniform, or standard roughness such as sandpaper that is applied over the leading-edge and stagnation point region may be an adequate representation of residual ice, but is likely too conservative in terms of maximum lift penalty. For some intercycle accretions, like those resulting from one-minute deicer cycles, the lift and drag penalties could be adequately simulated with uniform roughness. As the deicer cycle time increases from one to three minutes, intercycle ice shapes develop larger features that lead to more significant separated flow areas and larger performance penalties. Some may have characteristics of spanwise-ridge ice that are often simulated with simple geometric shapes. These results show a very large range of performance characteristics from increases in maximum lift to very large decreases in maximum lift. It is difficult to evaluate some of these results because the simple geometries used to represent the ice ridges do not capture the complexities of the actual ice accretion. More data are needed to better understand the flowfield physics.

I. Introduction

Comprehensive reviews of iced-airfoil aerodynamics and performance have recently been compiled.[1-3] These reviews have tended to focus on ice accretions that form on unprotected airfoil and wing surfaces. While this is an important area of icing research, aircraft certified for flight in icing conditions employ ice-protection systems (IPS) on the wing, tail and other components. In some cases, these ice-protection systems do not remove all ice on the airfoil/wing surface. The term "ice remnants" refers to this ice left over from the IPS operation. In the case of pneumatic systems, electro-expulsive systems, hybrid systems or even some heated systems that operate on a cycle, residual and intercycle ice are types of ice remnants. Residual ice has been defined as the ice that remains on the airfoil/wing immediately after the IPS has been activated.[4] Intercycle ice, on the other hand, refers to the ice that builds up on the airfoil/wing between cycles, immediately before the IPS activation.[5,6] Another type of ice remnant takes the form of a spanwise-running ridge.[4] Examples of this include runback ice in the case of bleed air or electro-thermal systems. For these systems any impinging water that does not evaporate runs downstream and freezes on an unheated portion of the airfoil/wing. Spanwise ridges may also form from water impingement and/or splashing downstream of the protected region. The purpose of this paper is to survey previous research on ice remnants and describe what is known about the resulting aerodynamics and performance and to identify where more research is required. Where possible, the aerodynamics are described from a flowfield-physics perspective.

The classification of iced-airfoil aerodynamics by flowfield physics is the subject of a recent review by Bragg et al.[3] The authors proposed four categories of ice accretion without regard to their formation, but instead, regarding their affect on the airfoil flowfield. The four categories: roughness, horn, streamwise and ridge result in different flowfield aerodynamics. Roughness is most often associated with initial ice accretion. Its primary effects are promotion of boundary-layer transition and removal of momentum from the boundary layer. This results in

* Research Scientist, Department of Aerospace Engineering, Senior Member AIAA.
† Professor and Head, Department of Aerospace Engineering, Fellow AIAA.

increased drag and trailing-edge separation that reduces the airfoil maximum lift coefficient ($C_{l,max}$). Horn ice usually results from glaze icing conditions and is characterized by the ice features that have surfaces nearly perpendicular to the oncoming flow. The horns result in large separation bubbles on the airfoil. The separation bubbles greatly increase the drag and reduce the lift. The unsteady aspects of the flow also result in force fluctuations and are very difficult to simulate computationally. Streamwise ice often results from rime icing conditions and is more conformal to the airfoil surface. While there is usually a small separation bubble on the airfoil, the stall is generally governed by trailing-edge separation instead of large bubble growth with increased angle of attack as in the horn case. Finally, the ridge-ice category has much relevance to ice remnants considered here because this is often runback ice or ice accretion resulting from water impingement downstream, or near the limits, of protected surfaces. The flowfield is dominated by a large separation bubble that forms downstream of the ridge. The aerodynamics are different from the horn ice case because the boundary layer develops on the airfoil surface upstream of the ridge. This means that the clean airfoil geometry plays a much larger role in determining the effect of the separation bubble on the flowfield and aerodynamic performance. This paper describes to what extent these categories may apply to ice remnants and considers where new categories may be needed.

Another recent review has considered icing effects on aerodynamic performance. Lynch and Khodadoust[1] have provided and an excellent and exhaustive review of the effect of ice accretion on performance parameters like lift and drag. They compiled nearly all available and relevant experimental aerodynamic performance data for various types of ice accretion and airfoil/wing geometries. The authors considered ice due to initial in-flight accretion, runback and ridge type accretion, large in-flight accretion and ground frost accretion. Of these categories, the initial accretion and ridge-ice shapes are the most directly related to the present topic of ice remnants. In yet another review of aircraft icing issues, Cebeci and Kafyeke[2] describe the challenges of predicting the geometry and surface extent of ice remnants. They point out the potential aerodynamic significance of these types of accretions from an aircraft certification perspective.

The purpose of this paper is to survey previous research on ice remnants and describe what is known about the resulting aerodynamics and performance. The paper describes the aerodynamic effects of ice remnants as they relate to the aerodynamic effects of standard roughness and other contamination. In addition, this review will help identify areas where more research is needed for a better understanding of the aerodynamics. Where possible, the aerodynamics are described from a flowfield-physics perspective. This approach follows the framework established by Bragg et al.[3] but also relies on compilation of performance data. After a brief historical review of ice-remnant research, performance data are discussed for the various types of ice remnants. It is important to note that this review is invariably flawed, as is any review associated with an active research area. While this review briefly summarizes our current understanding, continued research will, inevitably, modify and refine the ideas presented here. This is especially true in the present case, since ice-remnant research has not been explored in nearly the same detail as ice accretion on unprotected surfaces. Further, the various types of ice-protection systems currently in use add another independent variable to an already complex problem.

II. Literature Review

The purpose of this literature review is not to provide a complete guide to all ice-remnant research, but to review some of the research known to the authors to be significant and representative in the history of ice-protection systems. The review includes added detail where the research considered aerodynamic effects. This is the most relevant to this paper. Since no new data were acquired for this study, the review of historical data is important as it forms the basis for the assessment of aerodynamic effects.

Some of the earliest ice-remnant research was performed by the National Advisory Committee for Aeronautics (NACA) and dates back to the 1950s. In 1953, Gray and von Glahn[7] documented runback-ice shapes and resulting aerodynamic performance effects for a NACA 65_1-212 airfoil equipped with a hot-air anti-icing system in the Lewis Flight Propulsion Laboratory Icing Research Tunnel. The thermal IPS was operated continuously at a temperature and mass flow rate that evaporated approximately 28 to 44% of the impinging water. The system was also operated in a periodic deicing mode using four-minute cycles. The authors documented the approximate size and location of runback ridges and the corresponding changes in airfoil drag, measured in-situ during the icing exposure using a wake rake. Gray and von Glahn also made an insightful attempt to interpret their drag data in terms of the aerodynamic penalties measured by Jacobs[8] for protuberances on an NACA 0012 airfoil. The authors realized that Jacobs's protuberance could be interpreted as a simulation of the runback-ridge ice accretion. They applied these data carefully to further estimate the detrimental performance effects resulting from the documented accretions.

Consistent with the understanding at the time, Gray and von Glahn echoed Jacob's result that the largest aerodynamic penalties were associated with ridges located in the "leading-edge radius region."

In 1956, Bowden[9] published a report on residual and intercycle ice effects associated with pneumatic deicers installed on a NACA 0011 airfoil model. Bowden recorded the changes in airfoil performance (lift, drag and pitching moment) using force-balance measurements over the course of an icing exposure with a periodic deicer cycling time. He investigated the effect of cycling times, operating pressure, inflation rates and the differences between deicers with spanwise tubes and chordwise tubes. After investigating a range of icing conditions, Bowden concluded that the ice-removal characteristics of spanwise and chordwise tube layouts were very similar and that each should be operated using one-minute cycles to obtain the minimum iced-airfoil drag. He showed that a steady-state accretion and shedding process was achieved after two or three deicer cycles. Following the work of Jacobs,[8] Bowden also tested simulated ice shapes in the form of spanwise protuberances, or spoilers. He correlated the most critical protuberance location (defined in terms of increased drag coefficient) with the location of the maximum local air velocity (minimum C_p) on the model. While both Bowden, and Gray and von Glahn, provided excellent reports on ice remnants and performance effects, they were limited to the aerodynamic performance measurements that could be made. Their experimental apparatus was not able to accurately determine the effect of the ice remnants on maximum lift—a critical flight safety parameter.

With the commencement of the space program in 1959, icing research in the United States was mainly conducted in the private sector and any research on the effects of ice remnants was, and remains, propriety. Icing research was reinvigorated at NASA in the late 1970s and work on ice remnants also resumed. For example, Albright et al.[10] published a report in 1981 on the application of a pneumatic deicing system to a general aviation wing. Similar to the aforementioned studies, drag measurements were conducted in-situ during the icing tests. The drag increases due to residual and intercycle ice formation were similar in magnitude to the previous reports.

In the early 1990s engineers at NASA conducted a comprehensive study of low-power deicing systems.[11-14] Eight different deicing systems were investigated in the NASA Lewis Icing Research Tunnel (IRT), using a 21-inch chord NACA 0012 airfoil at $\alpha = 4$ deg. for both rime and glaze icing conditions. Four of these were various types of pneumatic systems while the other four were various forms of electric devices. Shin and Bond[12] reported residual and intercycle ice roughness heights on the leading edge and lower surface for seven of the eight systems using one-minute cycles. The residual ice thickness on the leading edge was zero (meaning that all of the ice was removed) for six of the seven systems tested in the glaze icing condition. In the rime icing condition the residual ice roughness heights ranged from $k/c = 0$ to 0.0066. On the lower surface, the residual roughness heights ranged from $k/c = 0.0005$ to 0.0043 for the glaze icing condition and $k/c = 0.0005$ to 0.0033 for the rime icing condition. In contrast to this, the intercycle ice heights were significantly larger. For example, the measurements on the leading edge ranged from $k/c = 0.0022$ to 0.0103 for the glaze icing condition and $k/c = 0.0009$ to 0.0067 for the rime icing condition. While the NASA studies provide excellent documentation about the residual and intercycle ice roughness characteristics, no aerodynamic data were acquired. Shin and Bond[12] also commented that the residual ice roughness observed may have significant aerodynamic effects, but that uniformly distributed roughness may not be an appropriate simulation.

Ice-remnant research continued in the 1990s with the Advanced General Aviation Transport Experiments (AGATE) program. This program was a cooperative effort among NASA, FAA, industry and universities to design an advanced general aviation aircraft. A task of the AGATE program was to investigate low-power deicing systems and the resulting performance effects of residual and intercycle ice. This led to a number of studies. Reichhold and Bragg[15] reviewed previous research in this area and concluded that the aerodynamic effects could be significant for the AGATE aircraft design. An icing-tunnel test program was conducted to evaluate residual and intercycle ice characteristics for four different low-power deicing systems installed on an NLF 0414 airfoil model. The aerodynamic performance effects were reported by Jackson and Bragg,[16] Jackson[17] and Gile-Laflin and Papadakis.[18] Jackson and Bragg[16] tested various roughness simulations and two-dimensional representations of the intercycle ice accretions. Gile-Laflin and Papadakis[18] tested three-dimensional castings made from molds of the intercycle accretions. Both studies documented the reductions in lift and increases in drag for angles of attack up to and including stall.

Further research into residual and intercycle ice accretions was continued in the early 2000s for a conventional pneumatic system. A cooperative program involving FAA, NASA, University of Illinois and industry was established to document residual and intercycle ice characteristics and aerodynamic effects on a NACA 23012 airfoil model equipped with a pneumatic deicer. Details regarding the ice accretion testing are given in references 6 and 19. Aerodynamic testing of selected intercycle shapes was performed using castings made from molds of the

ice accretions. These data are given in references 5, 6 and 19. The maximum lift penalties for intercycle ice accretions resulting from three-minute deicer cycles were found to be on the order of 60%, while the increase in minimum drag was about 270%. Sandpaper roughness (40 and 80-grit) was also tested and resulted in about a 30% reduction in maximum lift and a 57% increase in minimum drag. The sandpaper roughness was not an accurate simulation of the intercycle ice shapes, as it did not accurately represent the ice thickness and ridge-like characteristics. In a follow-on study by Broeren and Bragg,[20] built-up roughness simulations were tested on smaller scale NACA 23012, NACA 3415 and NLF-0414 airfoils. The performance data for the NACA 23012 airfoil matched the previous results with the ice castings simulations fairly well, thus indicating that the built-up roughness simulations were adequate. These roughness simulations were applied to the other two airfoils and the performance degradations were found to be less severe than for the NACA 23012 airfoil. This result was consistent with previous understanding of the effects of airfoil geometry and surface-pressure distribution.

The 1994 Roselawn ATR-72 accident has focused an enormous amount of research on super-cooled, large-droplet (SLD) ice accretion and performance effects. Miller et al.[21] and Addy et al.[22] conducted ice accretion testing in the NASA IRT for full-scale Twin Otter and NACA 23012 wing sections equipped with pneumatic deicers. They found that a common characteristic of the intercycle ice was a spanwise-running ridge located near the downstream edge of the active portion of the deicer on both upper and lower surfaces. Some runs performed at total temperatures near 32 deg. F also resulted in runback type ice formations downstream of the active portion of the deicer. As the temperature was decreased, a more well-defined ridge formed near the active edge of the deicer and became more uniform spanwise and less prone to self-shedding. The ridge heights on the upper surface of the Twin Otter wing ranged from $k/c = 0.004$ to 0.010. The range was much larger on the NACA 23012 wing, from $k/c = 0.0$ to 0.0277. Addy et al.,[22] did measure some limited performance data for a subset of these runs in the IRT.

The aerodynamic effects of spanwise-running ridges were investigated by Lee and Bragg[23,24] using simple geometric simulations of various sizes and shapes on both NACA 23012 and NLF 0414 airfoils. The ice-shape step heights ranged from $k/c = 0.0056$ to 0.0139 and four different geometries were tested. This work led to a new understanding of the primary effects of ice-shape size and location on airfoil lift and drag. Another important consideration was the pressure distribution of the clean airfoil. This work culminated in review articles[25,26] that also include data for tests run on more airfoils. Similar experiments were carried out by Calay et al.[27] using $k/c = 0.0035$ shapes on a NACA 0012 airfoil to simulated runback ridges at three locations, $x/c = 0.05$, 0.15 and 0.25. Their results indicated that a ridge of this size can increase maximum lift and delay stall when located at $x/c = 0.15$ and 0.25. Reductions in maximum lift occurred when the shapes were tested at $x/c = 0.05$. A large range of geometries and sizes of ridge-ice shapes were also tested by Papadakis and Gile-Laflin[28] on a modified NACA 63_A-213 airfoil section. Results similar to Lee and Bragg[23-26] and Calay et al.[27] were obtained. While these studies provide valuable insight into the size, shape, location and airfoil-type effects an important consideration is that they were all performed with relatively simple (and two-dimensional) simulations of ridge-type ice accretion. Bragg et al.[3] point out that spanwise variations in this type of ice accretion are large and could result in correspondingly large variation in the integrated performance.

The most recent study of runback ridge-type accretions was performed under a joint NASA and FAA program. Whalen et al.[29] conducted icing-tunnel testing on a business jet wing model equipped with a bleed-air based thermal IPS. Runback-ice ridge geometries were documented for three simulated flight cases. These shapes were scaled down and simulated for aerodynamic testing on NACA 23012 and 3415 airfoils. The step heights ranged in size from $k/c = 0.0035$ to 0.007. For some cases, the simulations were built-up with roughness to more closely mimic the actual ice accretion. This was an attempt to incorporate some higher level of simulation fidelity that had not been used in the previous studies.

This literature survey has covered the publicly available reports known to the authors to be significant contributions to the aerodynamics of ice remnants. Relative to the numbers of studies cited by Lynch and Khodadoust[1] and Bragg et al.,[3] this is certainly a small number. The following analysis of these data further reinforces this point. In spite of this, the exercise remains an important one in terms of guiding future experiments based on priorities for the required data.

III. Aerodynamic Effects of Ice Remnants

As the historical review has shown, ice remnants can take many forms ranging from small roughness to larger intercycle accretions to spanwise-running ridges. A goal of this paper is to understand the aerodynamic similarities and differences among these cases. The following discussion is organized by the type of ice remnant. Effects of residual ice are considered first and then compared with the effects of intercycle ice. A discussion of roughness is

included because this is often used in practice to simulate residual and intercycle ice accretions for aerodynamic testing. The effect of spanwise-ridge type ice shapes is then presented. Finally the discussion concludes with a comment on Reynolds number effects.

A. Residual Ice

Residual ice is defined as the ice that remains on the airfoil surface immediately after the activation of a deicing system, during steady-state cycling operation. For most systems documented in the literature, this means that the leading-edge region is cleared of ice downstream to some location that is dependent upon many factors. This is illustrated in Fig. 1 for a NACA 23012 airfoil equipped with a pneumatic deicing system. The maximum height of the upper surface ice was $k/c = 0.006$. A majority of the residual ice was much smaller than this. This maximum height was similar to the upper range of the data reported by Shin and Bond[12] for tests on the NACA 0012 airfoil. An examination of the pictures in the Bowden[9] report are qualitatively similar to these studies, but since no measurements were provided, it is impossible to be sure that the heights were in the same range.

The available aerodynamic data are perhaps even more limited. Bowden's measurements were conducted at only a few of angles of attack and were limited by the large model size. An example of this, given in Fig. 2, shows that in nearly all cases, except for high liquid-water content, the residual ice resulted in drag coefficients lower than for the airfoil with NACA standard roughness. According to Abbott and von Doenhoff,[30] the standard roughness had $k/c = 0.00046$ and covered $x/c = 0.0$ to 0.08 on both upper and lower surfaces. Based upon the previous residual ice measurements, it can be assumed that Bowden's residual ice thickness was at least this large, if not many times larger.

The Bowden[9] data in Fig. 2 were extracted and combined with data from an unpublished roughness study conducted at the University of Illinois. The roughness study was performed on a modified NACA 63-series airfoil and an NLF 0414 airfoil. The roughness had a range of k/c from 0.0006 to 0.0028 and was placed on the upper and lower surface downstream of the leading edge. Therefore, this could be considered a simulation of residual ice. A summary of the effect on drag coefficient is shown in Fig. 3. The increase in C_d from the clean, or smooth, airfoil is plotted against the clean, or smooth, airfoil C_l. In the case of Bowden's data, the clean value of the drag was taken for the "smooth" airfoil from Abbott and von Doenhoff.[30] This was done so that the results would be consistent with those from the roughness study on the other two airfoils. Figure 3 shows that the increase in drag for the NACA 0011 was at most 0.004, while the minimum increase in drag was 0.005 for the other two airfoils. Since the size of the residual ice roughness on the NACA 0011 is unknown, it is virtually impossible to determine if this difference in drag rise was due to roughness size, location or other factors.

Also shown in Fig. 3 is a similar plot for boundary-layer trips located on the upper and lower surfaces. This plot is included to show that some effects of residual ice, especially the Bowden[9] data, may be similar to boundary-layer trips placed near the leading edge. As a result, the effects on maximum lift would also be expected to be fairly small. In the case of the boundary-layer trip configurations, there was virtually no change in $C_{l,max}$.[6,31,32] Figure 4 summarizes the effect on lift for the NLF 0414 residual ice simulations. For this airfoil, there are significant deviations in C_l in the linear range of the lift curve due to its rather unusual separation characteristics (see Jackson[17] for more details on this behavior). However, the decrease in $C_{l,max}$ is less than 0.10. Even smaller differences in lift coefficient were observed for the roughness tested on the modified NACA 63-series airfoil. While the performance effects of residual ice roughness are fairly small, and may well be acceptable for aircraft operations, the lack of data naturally raises concerns about the universality of these effects. Therefore, it is recommended that more research be carried out to investigate roughness effects where the leading-edge radius region of the airfoil is assumed to be smooth, or free of roughness.

An important factor in determining the aerodynamic effects of residual ice is quantifying the height of residual ice roughness relative to the local boundary-layer thickness. Figure 5 shows boundary-layer thickness variation with chordwise location for the NACA 23012 and NLF 0414 airfoils at various Reynolds numbers. These data were obtained from a Faulkner-Skan calculation as described by Whalen et al.[33] As expected, the boundary layer is very thin in the area of the stagnation point and grows thicker downstream. Since initial ice accretion on an unprotected surface, or before an IPS is activated, forms about the stagnation point the roughness is easily many times larger than the boundary-layer thickness. In contrast, the stagnation point region is usual clear of ice immediately after IPS operation and the residual ice can be located a few to several percent chord downstream. Figure 5 shows that the smaller sizes of residual ice roughness may be on the order of the boundary-layer thickness, especially several percent chord downstream of the leading edge. With the area around the stagnation point clear of ice, the boundary layer develops some thickness before encountering the roughness. This may explain why the NACA standard

roughness resulted in higher drag for many of the cases in Fig. 2. Since the standard roughness covered the leading edge, the boundary layer was forced to develop over the roughness from the stagnation point on downstream.

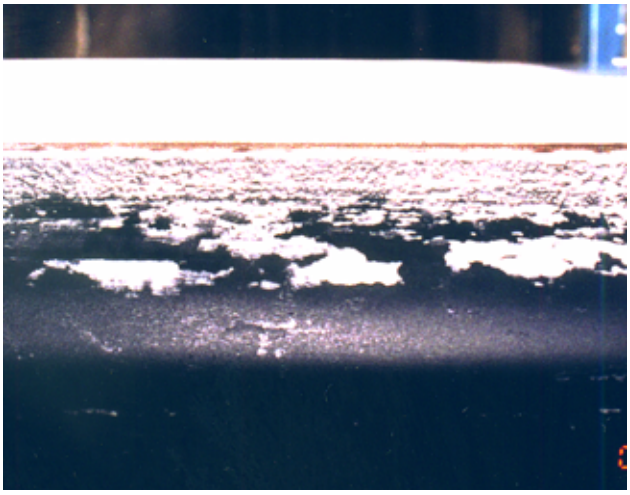

Fig. 1 Photograph of residual ice accretion on the upper surface of a NACA 23012 airfoil equipped with a pneumatic deicer, taken from Broeren and Bragg.[6]

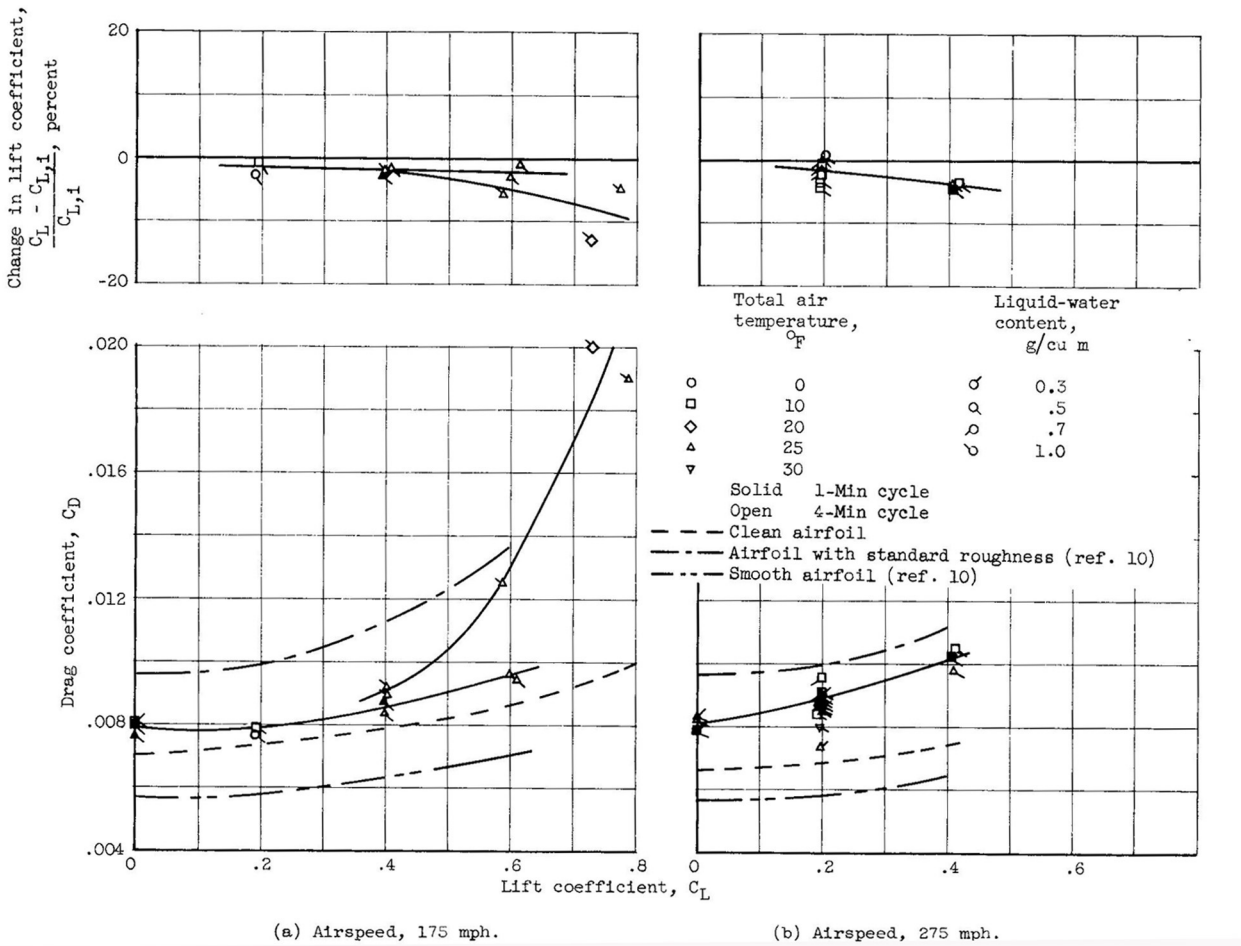

Fig. 2 Effect of residual ice on lift and drag for a NACA 0011 airfoil equipped with a pneumatic deicer at *Re* = 12×10^6 and 19×10^6 and *M* = 0.24 and 0.38, taken from Bowden.[9]

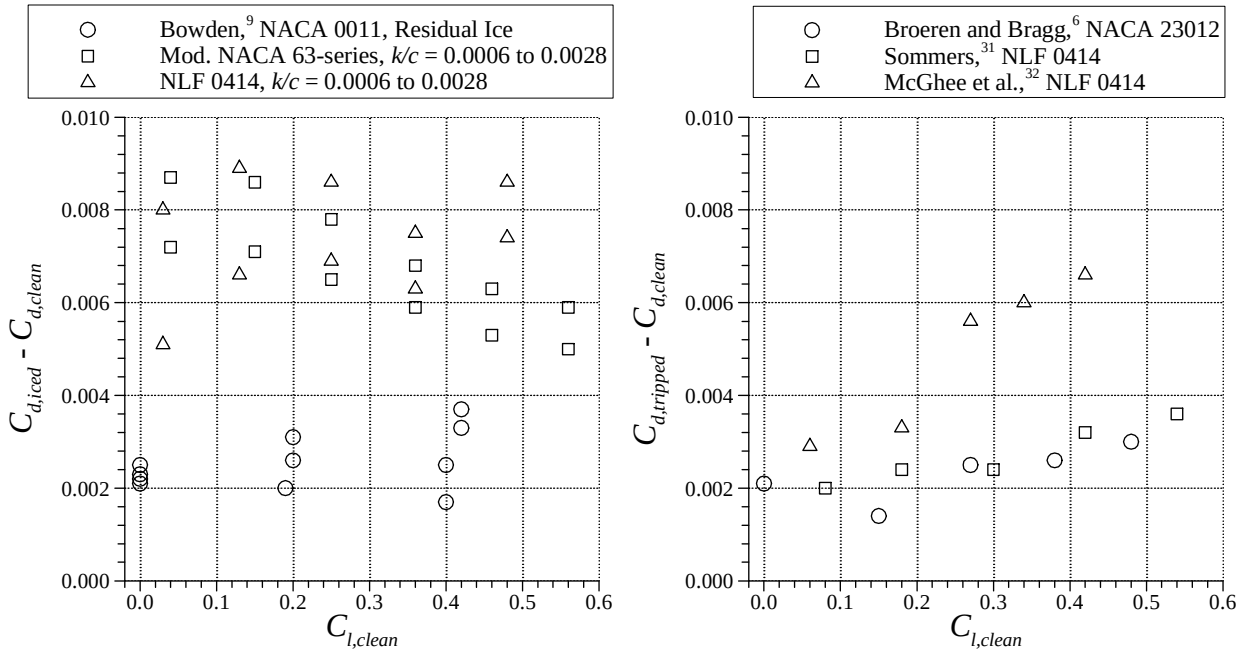

Fig. 3 Effect on airfoil drag due to residual ice roughness (left) and boundary-layer trips. Bowden[9] data at $Re = 12\times10^6$ and 19×10^6, $M = 0.24$ and 0.38. Roughness on modified NACA 63-series and NLF 0414 applied downstream of the leading edge on both upper and lower surfaces with $k/c = 0.0006$ to 0.0028 at $Re = 1.8\times10^6$ and $M = 0.18$. Upper and lower-surface boundary-layer trips: Broeren and Bragg[6] at $Re = 7.5\times10^6$ and $M = 0.12$, Sommers[31] at $Re = 3.0\times10^6$ and $M = 0.10$, and McGhee et al.[32] at $Re = 6.0\times10^6$ and $M = 0.10$.

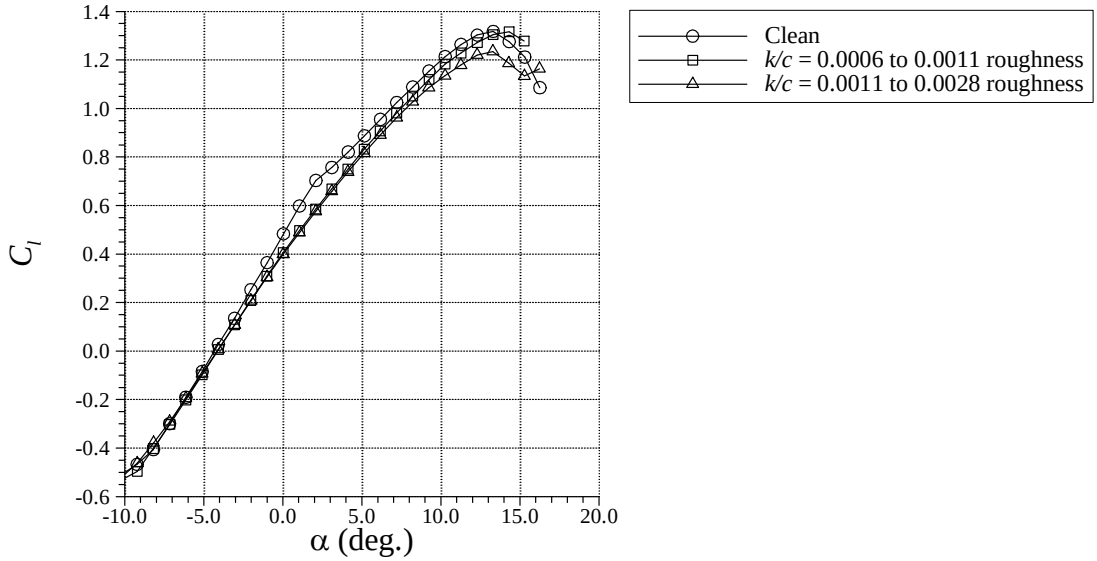

Fig. 4 Effect of simulated residual ice roughness on NLF 0414 airfoil lift at $Re = 1.8\times10^6$ and $M = 0.18$. Roughness applied downstream of the leading edge on both upper and lower surfaces.

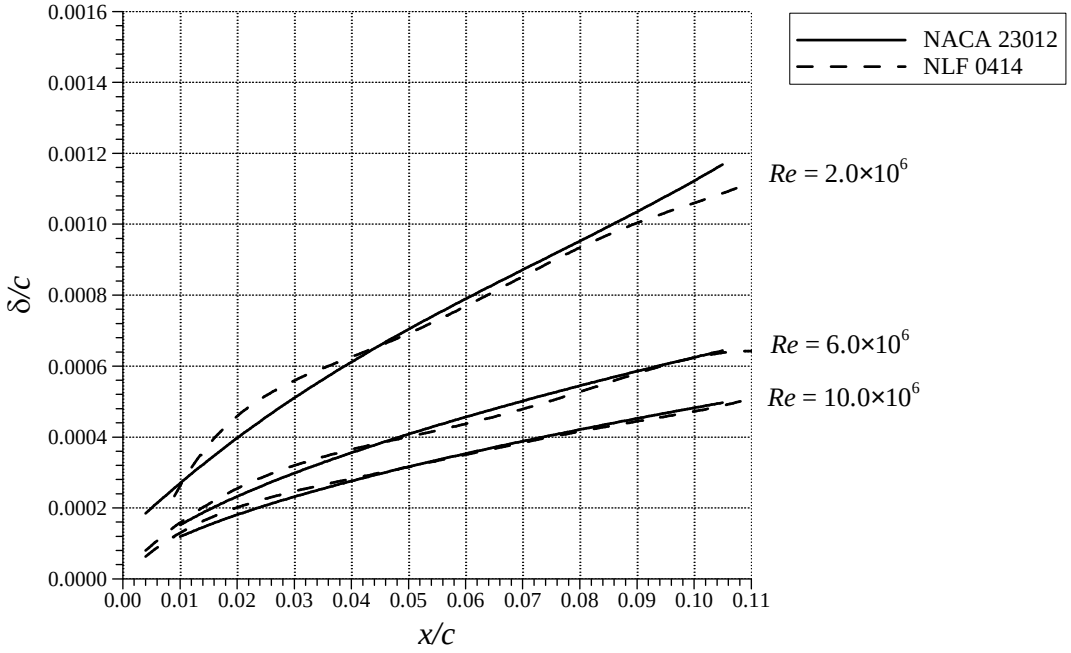

Fig. 5 Boundary-layer thickness versus chordwise location for NACA 23012 and NLF 0414 airfoils at three different Reynolds numbers. Data shown are for C_l = 0.4 with M = 0.2.

As discussed by Bragg et al.,[3] ice roughness that is much larger than the local boundary-layer thickness results in transition to turbulence via bypass mechanisms that are not clearly understood. The roughness itself extracts momentum from the boundary layer and outer flow. The combined effects result in higher drag and a tendency for boundary-layer separation to occur near the airfoil trailing edge at lower angle of attack than in the clean configuration. While some of these flowfield characteristics may apply to residual ice roughness, the data do not rule out the possibility of other effects, such as those that apply to boundary-layer trips. Since there are even less available flowfield data than performance data it is difficult to draw firm conclusions about the nature of the flowfield.

B. Intercycle Ice

Intercycle ice is defined as the ice that is present on the airfoil immediately before activation of a deicing system, during a steady-state cycling operation. Not only are the characteristics of this ice affected by the atmospheric conditions, but a primary factor is the time between activations. Usually, this time can vary from less than one minute up to three or four minutes. Depending upon this duration and the icing intensity, significant ice shapes can form in this interval. Yet the characteristics are different from initial ice accretion owing to the residual ice left behind from the cyclic operation. An example of an intercycle ice shape is shown in Fig. 6. Notice that the ice on the nose of the ice airfoil is relatively thin. However, there are a series of ice chunks that form a type of ridge near x/c = 0.06. This is just one example, and ice shapes from other studies exhibit a large variety of geometrical characteristics. Unlike the residual ice case, there are several studies that have considered the performance effects of intercycle ice.

The data summarized here are due to Gile-Laflin and Papadakis,[18] Jackson and Bragg[16] and Broeren et al.[5] In the first two studies, aerodynamic testing was carried out on an NLF 0414 airfoil. In Gile-Laflin and Papadakis,[18] castings of intercycle ice accretions were made from four different molds taken during icing-tunnel testing. The ice shapes were from four different ice-protection systems tested at the same icing condition. The authors diligently point out that these intercycle ice shapes were not considered representative of properly functioning ice-protection systems due to problems encountered during the ice accretion testing. However, it will be shown that the resulting performance degradations are not much different than in the other studies. Jackson and Bragg[16] tested four different intercycle ice simulations whose cross-sections were produced from tracings of the ice accretion during the various icing runs. The simulations were two-dimensional, that is, constant along the span of the aerodynamic model. This

also represented four different ice-protection systems operated at the same icing condition. Finally, Broeren et al.[5] also tested intercycle ice castings made from four different molds taken during icing-tunnel tests. In this case, a pneumatic IPS was used and the four different cases correspond to differences in icing conditions and deicer cycle time. These three studies yield performance data on 12 different intercycle ice simulations for two airfoils. To further facilitate comparison, all data were acquired within a Reynolds number range of 1.8×10^6 to 2.0×10^6.

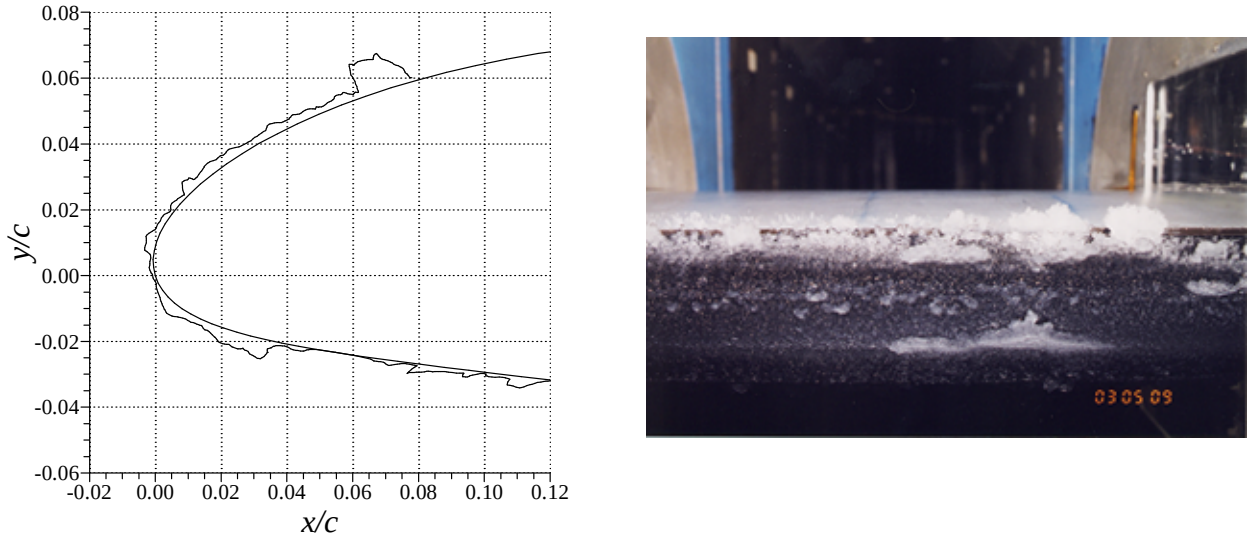

Fig. 6 Tracing and photograph of intercycle ice shape 312 on the upper surface of a NACA 23012 airfoil equipped with a pneumatic deicer, adapted from Broeren et al.[19]

The effect of the intercycle ice simulations on drag and maximum lift is shown in Fig. 7. First, note that the ordinate scale for the drag rise has been increased by a factor of 3.2 from the residual-ice drag plot shown in Fig. 4. As expected, the drag increases are much larger owing to both the increase in ice-shape size and the ice coverage over the whole leading-edge region. There appear to be two distinct groups of data in the figure. The set of points having the higher drag increase ($\Delta C_d > 0.016$) are for three of the four simulations tested on the NACA 23012. These three ice shapes were due to three-minute cycles of the deicer, whereas all of the other 9 ice shapes, corresponding to the lower drag values were due to one-minute deicer cycles.

The maximum lift data in Fig. 7 are plotted as a function of ice-shape height, which was estimated from the tracings for the largest ice feature on the leading-edge/upper-surface region of the airfoil. Therefore, the chordwise location of this "maximum height feature" varied across all of the ice shapes. The clean values for each airfoil are also indicated on the figure. There is a difference in the clean $C_{l,max}$ for the NLF 0414 airfoil from the two references, probably resulting from discrepancies between two models having different chord lengths tested in different facilities. However, the iced-airfoil data show a general trend of decreasing $C_{l,max}$ with increasing ice-shape height, as expected. The data also tend to reflect the difference in the one-minute and three-minute deicer operation as shown in the drag data. That is, the three lowest $C_{l,max}$ values (< 0.8) in Fig. 7 belong to the three three-minute intercycle ice shapes. Another consideration is that the decrease in $C_{l,max}$ from the clean value is the largest for the NACA 23012 with the intercycle ice shapes.

In another study, Broeren and Bragg[20] used built-up roughness simulations of the intercycle ice castings tested on the NACA 23012. The size and distribution of the roughness was designed to mimic the ice features shown in the castings. There were different built-up roughness simulations representing each of the four intercycle ice shapes. The relative success of this is shown in the lift data of Fig. 8. The comparison of $C_{l,max}$ between the castings and built-up roughness methods show good agreement for the NACA 23012. This provides some level of validation for the simulation method. The results for the same built-up roughness simulations tested on the NLF 0414 and NACA 3415 airfoils are also plotted. The $C_{l,max}$ values for the NLF 0414 that are less than 1.0 correspond to the simulations of three-minute cycle time accretions. Contrasted with the data in Fig. 7, these data may reflect the potential lift penalty between one-minute versus three-minute deicer cycles. Tests were performed on the NACA 3415 airfoil as

a way to gauge sensitivity to airfoil type. The data indicate iced-airfoil $C_{l,max}$ values within the spread of the other two airfoils. Relative to the clean maximum lift, the NACA 23012 experienced more severe degradations than the other airfoils owing to its larger clean value. A comparison of the drag rise data in Fig. 8 for the NACA 23012 airfoil indicates the difficulty in trying to simulate the ice castings with built-up roughness. The overall range of the drag rise is similar to that shown in Fig. 7, with the larger values corresponding to simulations of ice accretions due to the three-minute deicer cycle.

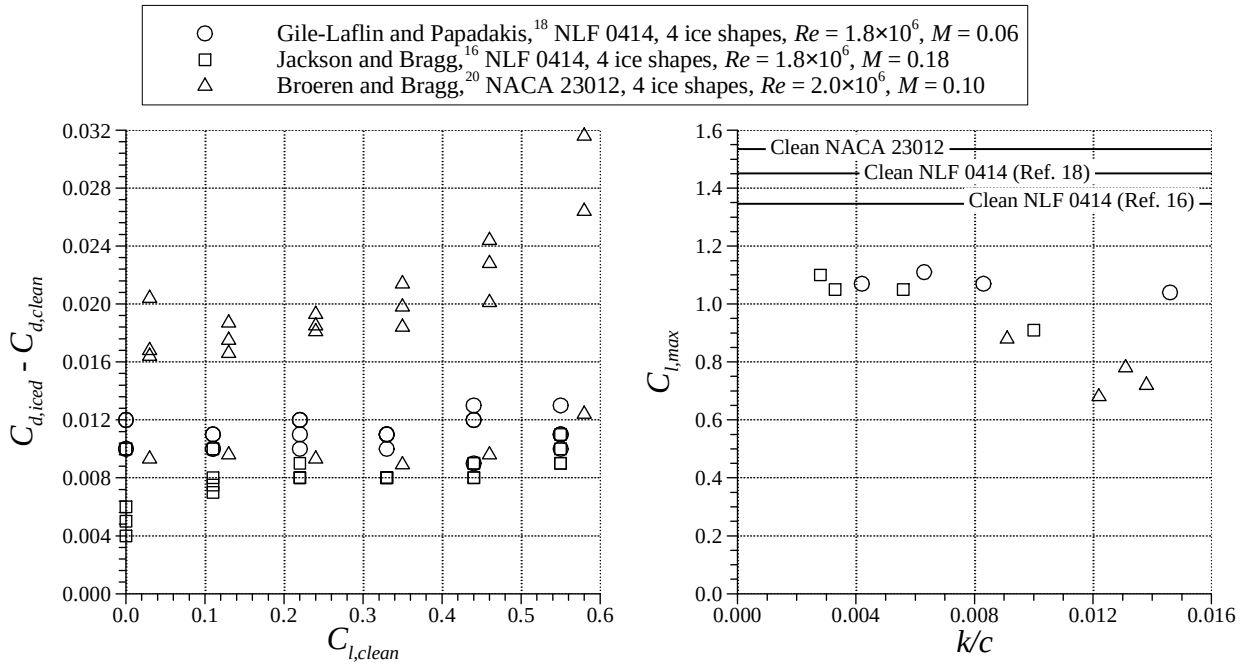

Fig. 7 Effect of simulated intercycle ice shapes on drag (left) and maximum lift.

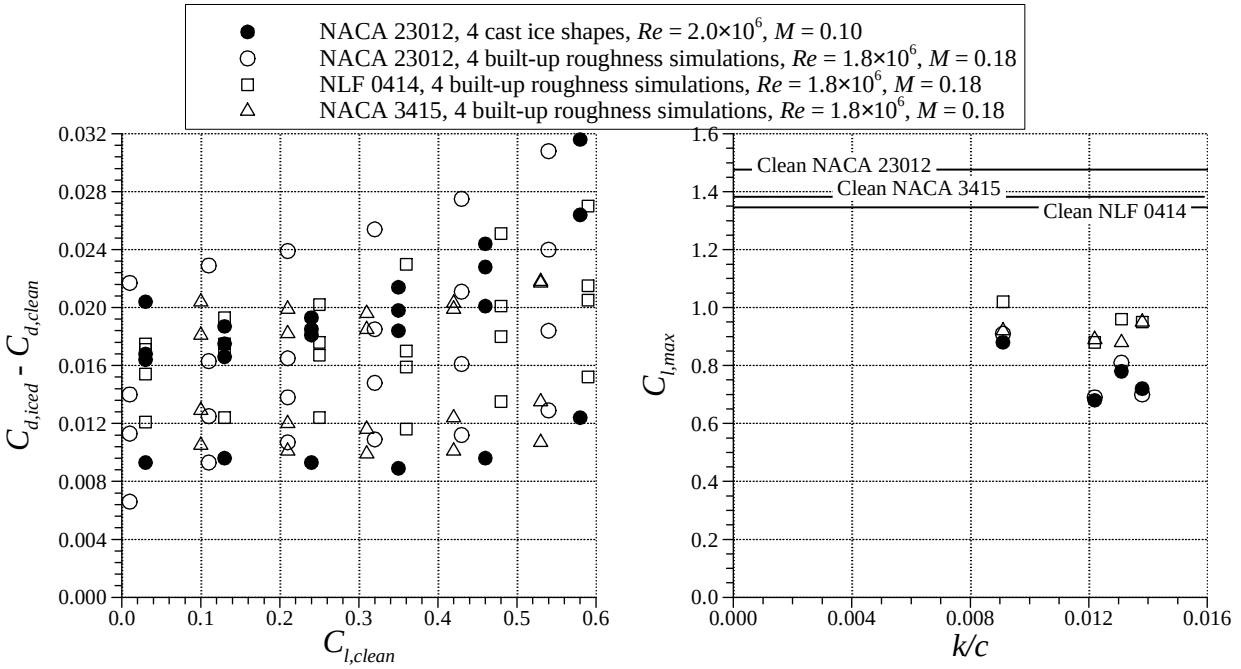

Fig. 8 Effect of built-up roughness intercycle ice simulations on drag (left) and maximum lift, for three airfoils, adapted from Broeren and Bragg.[20]

The general trends in the performance data shown here suggest that intercycle ice shapes may at least partially belong in the streamwise ice category of Bragg et al.[3] They defined characteristics of streamwise ice as having small areas of separated flow from the ice shape, but the main drivers of reduced lift and increased drag were thickening of the boundary layer and increased trailing-edge separation over the clean case. They further suggest that roughness added to "2D" streamwise ice simulations may increase drag, but have little effect on maximum lift. In fact, Jackson[17] demonstrated this for the intercycle ice shapes tested on the NFL 0414. Roughness added to the 2D smooth ice simulations did increase drag, but did not affect lift. The data in Fig. 8 for the NACA 23012 simulations tends to support this point as well. The built-up roughness simulations, mimicking the major ice features resulted in good comparison in $C_{l,max}$. But the differences in drag were larger because of inability of the built-up roughness to duplicate the roughness associated with the casting simulations. These data tend to indicate that some intercycle ice shapes may cause local flow separations on the scale of the ice features, but this flow separation probably does not govern the aerodynamics leading to stall. On the other hand, there is a large variation in the geometry of the intercycle ice accretions and some of the performance effects, especially for the NACA 23012, were large. This suggests that the extent of flow separation may be larger and that there is some overlap with the spanwise-ridge category of ice accretion discussed in section D. The fact that there exists such a large range of geometries and effects makes classification difficult. Flowfield data should be acquired for some of these cases to facilitate a better understanding of the stall mechanisms and how the ice accretions may be classified.

C. Uniform Roughness

Uniform roughness is not by itself a type of ice accretion or ice remnant. It is, of course, often used for simulating effects of initial, residual and intercycle ice accretion on airfoils. Lynch and Khodadoust[1] have compiled nearly all aerodynamic data for airfoils with (ice-like) roughness and provide an excellent summary. Therefore, the purpose here is not to review all of these results, but to select some cases for comparison to the residual and intercycle ice effects already discussed.

Roughness effects on airfoils are caused not only by the size and surface coverage of the roughness, but also by its shape and concentration.[3] These factors make aerodynamic comparison of roughness effects more difficult. Sandpaper is often used because its roughness size, shape and distribution is more tightly controlled and therefore is more uniform between different experiments. The effect of 40, 80 and 150-grit sandpaper roughness on airfoil performance is shown in Fig. 9 for NACA 23012 and NLF 0414 airfoils. The roughness sizes are k/c = 0.00114, 0.00046, 0.00023 for 40, 80 and 150-grit sandpaper, respectively. For the NLF 0414 airfoil, the roughness extended from x/c = 0.08 on the lower surface around the leading edge to x/c = 0.08 on the upper surface. For the NACA 23012, the roughness extended from x/c = 0.10 on the lower surface around the leading edge to x/c = 0.07 on the upper surface. The plot shows, for each airfoil at each C_l, the increase in drag penalty with increasing roughness size. The difference in the relative behavior of these trends for each airfoil at C_l's greater than 0.4 was due to the differences in the variation of the clean C_d with C_l. Compared to the data in Fig. 3, the effect of the sandpaper roughness on drag was similar to the residual ice roughness tested on the NLF 0414 and modified NACA 63-series airfoils. This was true despite the fact that the 80 and 150-grit sizes were smaller than the roughness of Fig. 3. That the drag results are similar is likely the result of the larger surface coverage of the sandpaper, particularly in the vicinity of the stagnation point, where the boundary layer was very thin.

The corresponding lift penalties demonstrate similar behavior to the one-minute intercycle ice shapes in Fig. 7. However, compared to the penalties for the built-up roughness simulations in Fig. 8, the sandpaper roughness result had considerably higher $C_{l,max}$. Since the few available data for residual ice maximum lift penalties indicate only minor effects, the sandpaper results are likely conservative in this regard. In terms of drag penalty, these results suggest that sandpaper roughness may be an adequate simulation for residual ice, but is likely inadequate for intercycle ice.

Another commonly used source of standard roughness data is that published for many NACA airfoils in Abbott and von Doenhoff.[30] This was "0.011-inch grain carborundum spread thinly to cover 5 to 10% of the leading edge to 0.08c on both surfaces." So, for the 24-inch chord models, this roughness had k/c = 0.00046. A key difference with sandpaper roughness is the concentration of the grit particles. The roughness concentration of sandpaper is basically 100% since the entire surface is covered. Bragg et al.[3] point out that for roughness of a given size, the maximum effect is achieved for concentrations near 30%, above which increasing the concentration has little additional aerodynamic effect. The lift and drag performance of this roughness for several airfoils is compared to sandpaper in Fig. 10. The sandpaper had k/c = 0.00057 (40-grit) and 0.00023 (80-grit) and was applied to the airfoil from x/c = 0.10 on the lower surface to 0.07 on the upper surface. The Abbott and von Doenhoff[30] data were at Re =

6.0×10^6 and the Broeren et al.[5] data were at $Re = 7.5\times10^6$. The data show that the NACA standard roughness tested on the various airfoils was comparable to the sandpaper effects. Also, there is good overlap with the data in Fig. 9, which have slightly higher ΔC_d and slightly lower $C_{l,max}$ values due to the largest k/c value (0.00114). The data are provided to show (1) the comparability of NACA standard roughness data to sandpaper roughness and (2) the relative insensitivity of Reynolds number in the airfoil-with-roughness data. More discussion on Reynolds number effects is given in Section IV.

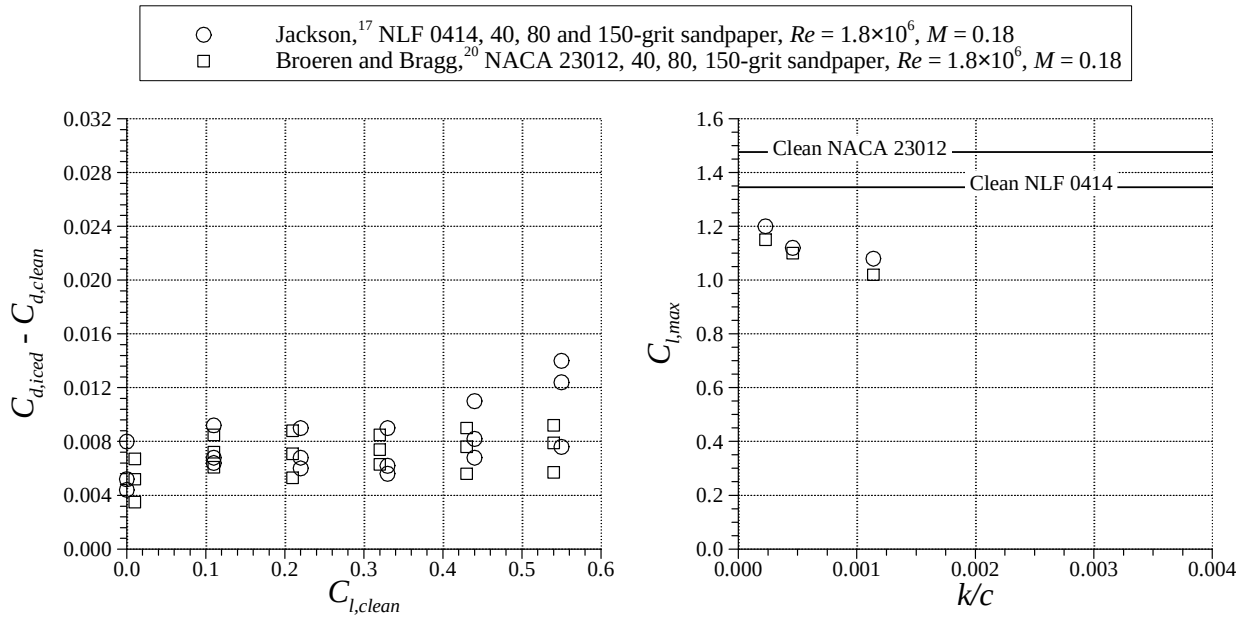

Fig. 9 Effect of sandpaper roughness on drag (left) and maximum lift. Coverage for NLF 0414 was from x/c = 0.08 on the lower surface to x/c = 0.08 on the upper surface. Coverage for the NACA 23012 was from x/c = 0.10 on the lower surface to x/c = 0.07 on the upper surface.

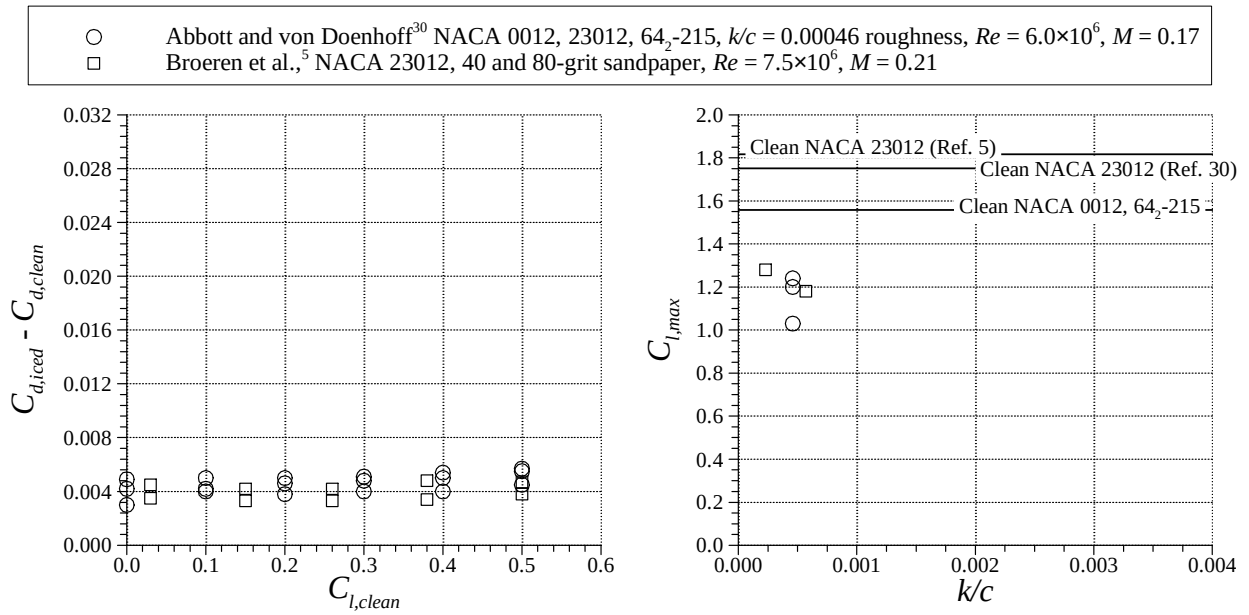

Fig. 10 Comparison of NACA standard roughness and sandpaper roughness effects on drag (left) and maximum lift. Coverage for NACA standard roughness (k/c = 0.00046) was from x/c = 0.08 on the lower surface to x/c = 0.08 on the upper surface. Coverage for the sandpaper roughness was x/c = 0.10 on the lower surface to x/c = 0.07 on the upper surface.

Further illustration of the comparative effects of uniform roughness with the residual and intercycle ice accretion is provided in Fig. 11. This is merely a combination of the data shown in Figs. 3, 7 and 9. Several points of discussion arise. The first point is that uniform roughness effects on drag seem to correlate with residual ice roughness effects, or are at least a conservative representation. However, the limited amount of maximum lift data indicate that the uniform roughness is likely very conservative relative to residual ice effects. This is not surprising given the differences in surface coverage. This means that uniform roughness may be an adequate simulation of residual ice. The problem is that the lack of detailed aerodynamic data may lead to exceptions. This possibility persists until a better understanding of the residual ice aerodynamics is obtained.

The data in Fig. 11 further indicate that uniform roughness may be suitable for simulating the performances effects of the one-minute intercycle ice accretions obtained on the NLF 0414. However, there exists the chance that the details of the roughness on an intercycle ice shape may have significant effects on the drag that simply cannot be modeled with uniform roughness, because of the differences in flowfield physics. As the cycle time increases to three minutes, the data clearly show that uniform roughness is no longer an acceptable simulation of intercycle ice by any measure. In terms of the ice categories developed by Bragg et al.,[3] intercycle ice may well represent the overlap region between roughness and streamwise ice as the areas of separated flow may be confined to small pockets in the vicinity of the ice features. There are some examples of intercycle ice that also exhibit spanwise-ridge like features in their geometry and performance effects. This implies that there may also be overlap with the spanwise-ridge category. It is recommended that flowfield data be acquired to determine what features govern the aerodynamics. For example, even simple surface-oil flow visualization would provide useful information about the extent of boundary-layer separation. This would help classify the ice shape characteristics and lead to a better understanding of the performance effects.

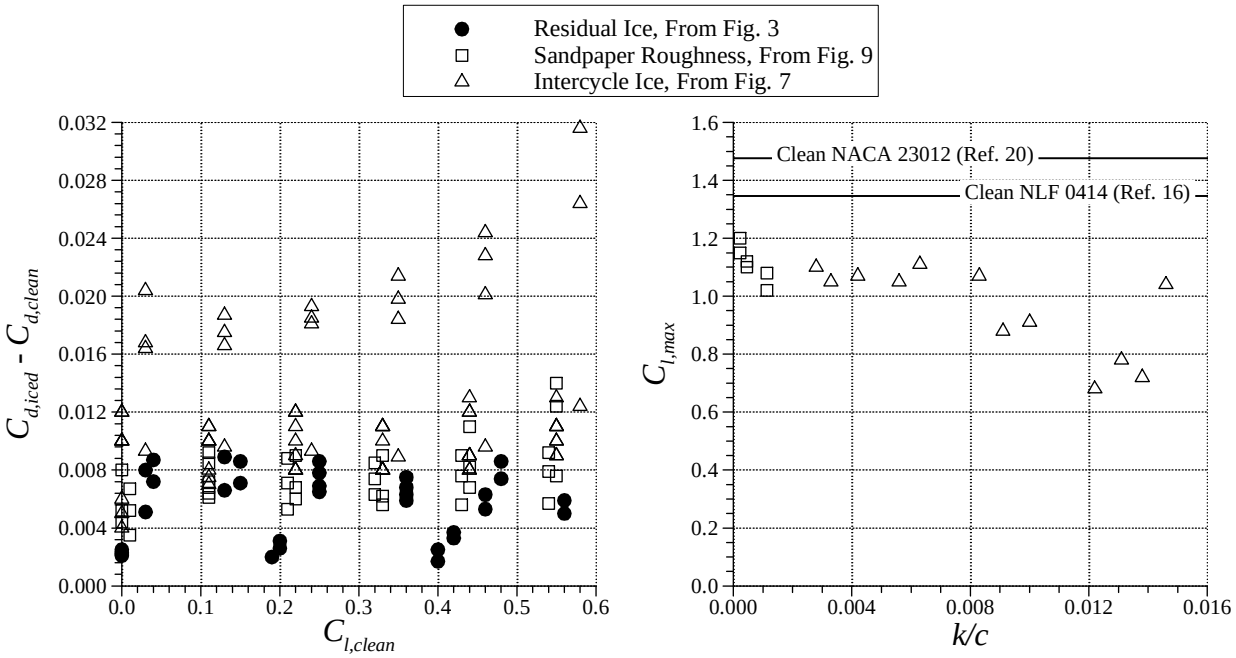

Fig. 11 Summary of residual ice, sandpaper roughness and intercycle ice effects on drag (left) and maximum lift. Data are identical to those in Figs. 3, 7 and 9.

The penalties in maximum lift shown here are mainly for the NACA 23012 and NLF 0414 airfoils. In virtually all cases, the iced-airfoil $C_{l,max}$ was lower for the NACA 23012 while having a higher clean value than the NLF 0414. The differences in sensitivity of these airfoils to ice accretions, particularly simulated ridge-type shapes has been addressed in other studies.[23,26] So there is no need to belabor this in detail, but some discussion is warranted. The NACA 23012 airfoil was designed for low-pitching moment. As a result, the pressure distribution has a large suction peak near the leading edge. In contrast, the NLF 0414 airfoil was designed for minimum drag over a certain C_l range. As a result, the pressure distribution is very uniform to maintain a long run of laminar boundary layer on the upper surface. For the NACA 23012 airfoil with leading-edge ice shapes, or roughness, the high suction

pressures on the leading edge cannot be achieved. The ice shapes, or roughness, also force a change of stall type to trailing-edge stall. The combination of these effects leads to the low values of $C_{l,max}$. The generation of lift on the NLF 0414 with leading-edge roughness or ice accretion can be maintained because the pressure distribution is more uniform, nor does this force a change in stall type. The combination of these factors for the NLF 0414 make it less sensitive to these accretions.

D. Spanwise-Ridge Ice

A separate category of ice remnants for spanwise-ridge ice was motivated, in part, by the differences in aerodynamics noted by Bragg et al.[3] for this type of accretion. The spanwise ridge forms downstream of the leading-edge radius region. In some cases, the airfoil surface upstream of the ridge is clear of ice. This leads to aerodynamic effects that can be very different from leading-edge accretions because the boundary layer develops ahead of the ridge. An example of this is shown in Fig. 12 for a wing model equipped with thermal IPS where the leading edge was continuously heated. Since not all of the impinging water evaporated, a runback ridge formed on the upper surface at $x/c \approx 0.16$ and had $k/c \approx 0.006$. The airfoil surface upstream was completely clear of ice and the lower surface also had a similar ridge. Clearly, this case is different from the previous examples of residual and intercycle ice accretion.

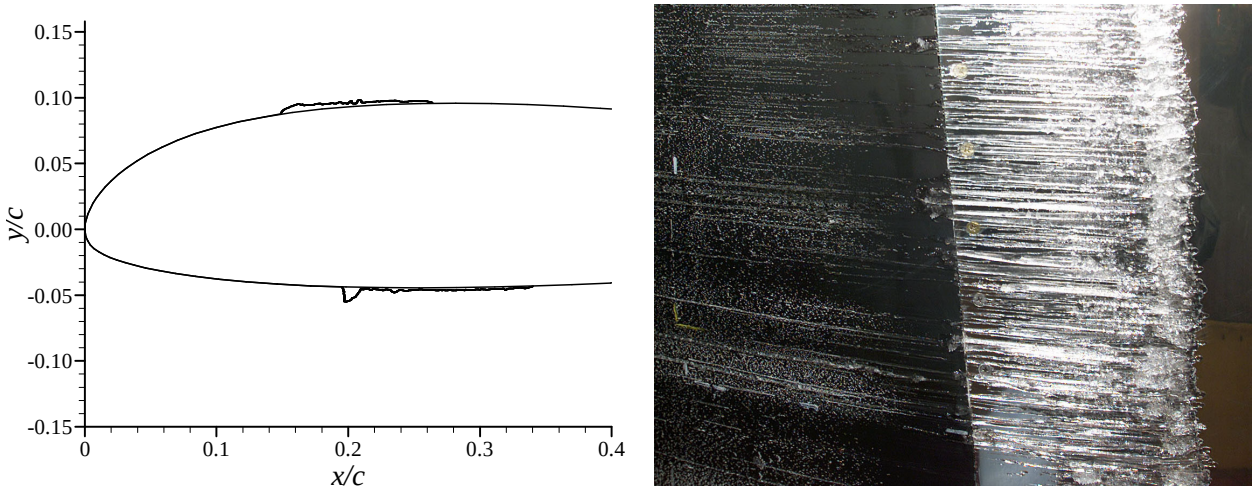

Fig. 12 Tracing and photograph of runback-ridge ice accretion on the upper surface of a business jet wing section equipped with a thermal anti-icing system, adapted from Whalen et al.[29]

Another common example of ridge-type ice accretion is associated with SLD conditions and with deicing systems. In SLD conditions, droplet impingement, splashing and runback water can occur downstream of, or near, the limits of the ice-protection systems. An example of this is shown in Fig. 13, taken from an icing-tunnel study of SLD accretions on a NACA 23012 wing section. The upper-surface ridge was located at $x/c \approx 0.06$ and had $k/c \approx 0.015$. By the present definitions, this could also be classified as intercycle ice, since it was documented immediately prior to a deicer activation. It is interesting to note that this is very similar to the intercycle ice example given in Fig. 6, which formed in smaller droplet, Appendix C conditions. In both cases the ridges were characterized by a large degree of spanwise variation in height, shape and location. In both cases, the resulting residual ice accretion would probably look similar since the ridges shed upon activation of the deicer. Therefore, there is some overlap in these categories. However, the majority of the spanwise-ridge aerodynamic studies only model the upper-surface ridge and not any other elements of the accretion. This simulation is often accomplished with a continuous, 2D shape.

Aerodynamic data obtained for actual ridge-type ice accretions, or high-fidelity simulations, such as castings, are very limited. Figure 14 summarizes the only data known to the authors that meet this requirement. The data on the NACA 23012 were acquired in the NASA IRT for the SLD type accretions shown in Fig. 13. These were measured at one angle of attack for various values of total temperature in the range of 5 to 34 deg. F. Addy et al.,[22] remind readers that these data should be interpreted carefully because they were obtained using a force balance and therefore represent the increment in drag over the entire model. However, the SLD icing cloud was nonuniform

outside of a one-foot area near the tunnel centerline. This resulted in ice accretion that tapered off significantly near the tunnel walls. Because of this, it is likely that the actual drag increments were larger. Despite this, it is interesting to note that these increments in drag are not substantially larger than those shown for other intercycle ice accretions in Fig. 7.

The NACA 65_1-212 data were also measured in the IRT using a wake rake. These were obtained by Gray and von Glahn[7] for runback ridges resulting from tests on a thermal IPS. The ridges were located at $x/c \approx 0.12$ and had $k/c \approx 0.0013$ to 0.002. In this case the drag penalty was on the order of the residual ice and boundary-layer trips shown in Fig. 3. The data in Fig. 14 illustrate the potential for large variation in the performance for these types of accretions.

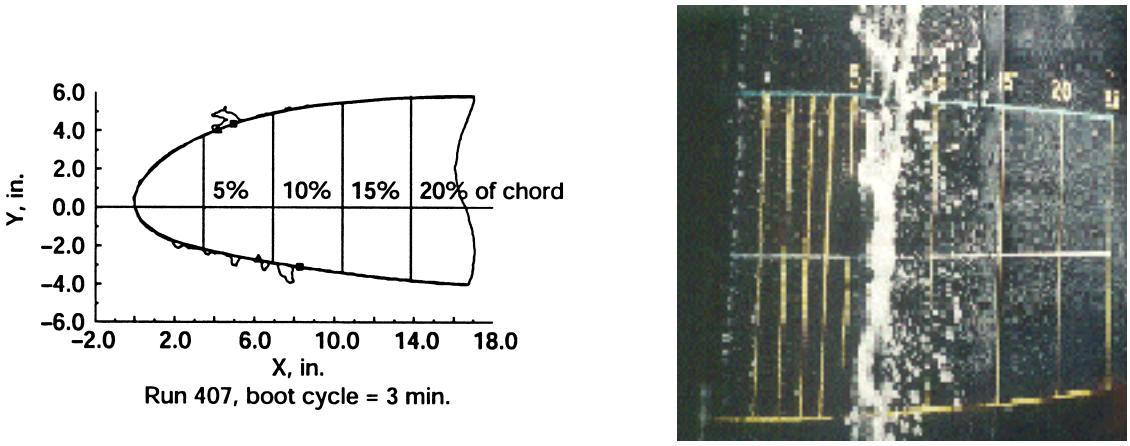

Fig. 13 Tracing and photograph of SLD ridge-type ice accretion on the upper surface of a NACA 23012 wing section equipped with a pneumatic deicer, adapted from Addy et al.[22]

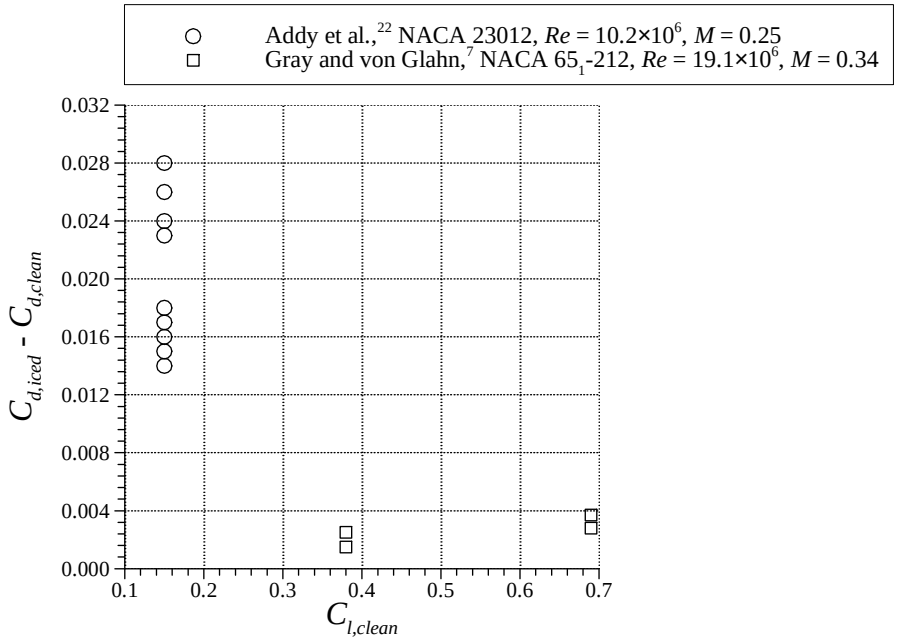

Fig. 14 Effect of spanwise-ridge ice accretion on drag as measured in icing-tunnel experiments.

Most other aerodynamic studies use very simple geometries to model spanwise-ridge ice accretions and only model the upper-surface ridge. One study that makes an attempt to fully simulate the aerodynamic effects of runback ridge ice is due to Whalen et al.[29] The authors simulated runback shapes obtained in an icing test, such as that shown in Fig. 12, with simple materials and combinations of roughness. These features were geometrically

scaled from the icing-tunnel model down to smaller size aerodynamic models with NACA 23012 and NACA 3415 airfoils. Two different cases were tested. In the first case, similar to Fig. 12, the upper and lower-surface ridges were located at $x/c = 0.16$ and $x/c = 0.20$, respectively and had heights from $k/c = 0.0035$ to 0.005 and $k/c = 0.008$ to 0.014, respectively. The second case resulted from much colder temperatures which resulted in the ridges being located closer to the leading edge. The upper and lower-surface ridges were located at $x/c = 0.015$ and $x/c = 0.035$, respectively and had heights from $k/c = 0.005$ to 0.007 and $k/c = 0.006$, respectively.

The aerodynamic results for the first case are plotted in Fig. 15 along with data from other studies. Papadakis and Gile-Laflin[28] tested simple triangular and spoiler geometries on a modified NACA 63_A-213 airfoil. These had $k/c = 0.0041$ and 0.0053, respectively, and were located at $x/c = 0.15$ on the upper surface only. Bragg and Loth[34] tested a forward-facing quarter-round on a NACA 23012m airfoil that had $k/c = 0.0056$ and was located at $x/c = 0.14$ on the upper surface only. Also included in Fig. 15 are the classic protuberance data on the NACA 0012 due to Jacobs.[8] The protuberance had a spoiler-type geometry with $k/c = 0.005$ and was located at $x/c = 0.15$ on the upper surface only. Therefore, Fig. 15 is a summary of the performance effects of these various geometries tested on various airfoils. Care has been taken to match, as closely as possible, the size and location of the ridges. Therefore, the differences in performance were due to ridge geometry and clean airfoil geometry.

The data show that the drag penalties for the Whalen et al.[29] simulations were higher than most other cases. This probably results from the fact that they also tested a lower-surface runback ridge in addition to the upper-surface ridge. This, of course, is more realistic and probably more accurately reflects the true drag penalty of a runback-type ridge accretion. In this case, the drag rise for the ridge shapes was generally larger than for the three-minute intercycle accretions shown in Fig. 7. The data show that if only an upper-surface ridge is present, the drag penalty could be in the range of small intercycle ice accretions.

The effect on maximum lift also shows a large variation. The simulated runback ice shapes tested by Whalen et al.[29] had nearly the same $C_{l,max}$ for both airfoils. This meant that the NACA 23012 experienced more of a reduction due to its higher clean $C_{l,max}$ value. However, the iced $C_{l,max}$ in this case was much larger than the NACA 23012m with the forward-facing quarter round. The lower-surface ridge present in the Whalen et al.[29] simulations was not expected to affect the $C_{l,max}$. So the major differences in the upper-surface ridge between the two studies was geometric. That is, the Whalen et al.[29] ridge had a substantial chordwise extent (from $x/c = 0.16$ to ≈ 0.24) with spanwise variations in height due to the addition of grit roughness. The Bragg and Loth[34] ridge was a simple forward-facing quarter round. It is possible this difference in geometry resulted in the large difference in $C_{l,max}$ shown in Fig.15. Bragg et al.[3] point out that the cross-sectional and spanwise geometry of ridge ice shapes are very important factors in the resulting aerodynamics.

In the case of the Papadakis and Gile-Laflin[28] data, the maximum lift performance was improved by the addition of the ridge shapes over the clean model case. Such results are similar to those obtained by Calay et al.,[27] who tested $k/c = 0.0035$ triangular shapes on a NACA 0012 airfoil at $x/c = 0.15$ and $Re = 1.25\times10^6$. (These data were not plotted here because of model size limitations in that experiment.) Yet, a change of geometry to a spoiler protuberance, an increase of k/c to 0.005 and an increase in Re to 3.1×10^6, tested by Jacobs[8] on a NACA 0012 resulted in a $C_{l,max}$ reduction. This sensitivity of $C_{l,max}$ due to similar spanwise-ridge shapes is currently being explored by Whalen et al.[33] The local boundary-layer thickness for larger angles of attack at $x/c = 0.15$ to 0.16 on the upper surface can be on the same order of magnitude as the ridge heights tested. Therefore, it is not surprising that the small range of ridge heights shown in Fig. 15 have such large differences in performance. With ridge heights approaching the boundary-layer thickness, the effects of ridge geometry, airfoil geometry and Reynolds number all become much more important to the resulting aerodynamics. Unfortunately, there is little flowfield data known to the authors that would provide more insight into these effects.

The aerodynamic effect of the second set of runback ridge simulations tested by Whalen et al.[29] is shown in Fig. 16 along with data from other studies. The $k/c = 0.0041$ triangular geometry was tested by Papadakis and Gile-Laflin[28] at $x/c = 0.025$. Bragg and Loth[34] tested the $k/c = 0.0056$ quarter-round geometry at $x/c = 0.02$. The drag results are similar to Fig. 15, where the Whalen et al.[29] data had the largest drag penalty owing to the presence of the lower-surface ridge. It is interesting to note that this drag penalty was less than for the ridges located much farther downstream and that it was closer in magnitude to the three-minute intercycle ice accretions shown in Fig. 7. The difference in the Whalen et al.[29] drag data may have also been due to differences in geometry between the simulations in Figs. 15 and 16. The maximum lift reductions resulting from these ridge geometries are more typical of leading-edge ice shapes. That is, no increases in $C_{l,max}$ were observed. It is also noteworthy that the range of $C_{l,max}$ in this case is also similar to the range shown in Fig. 7 for the intercycle ice shapes. With these ridge shapes

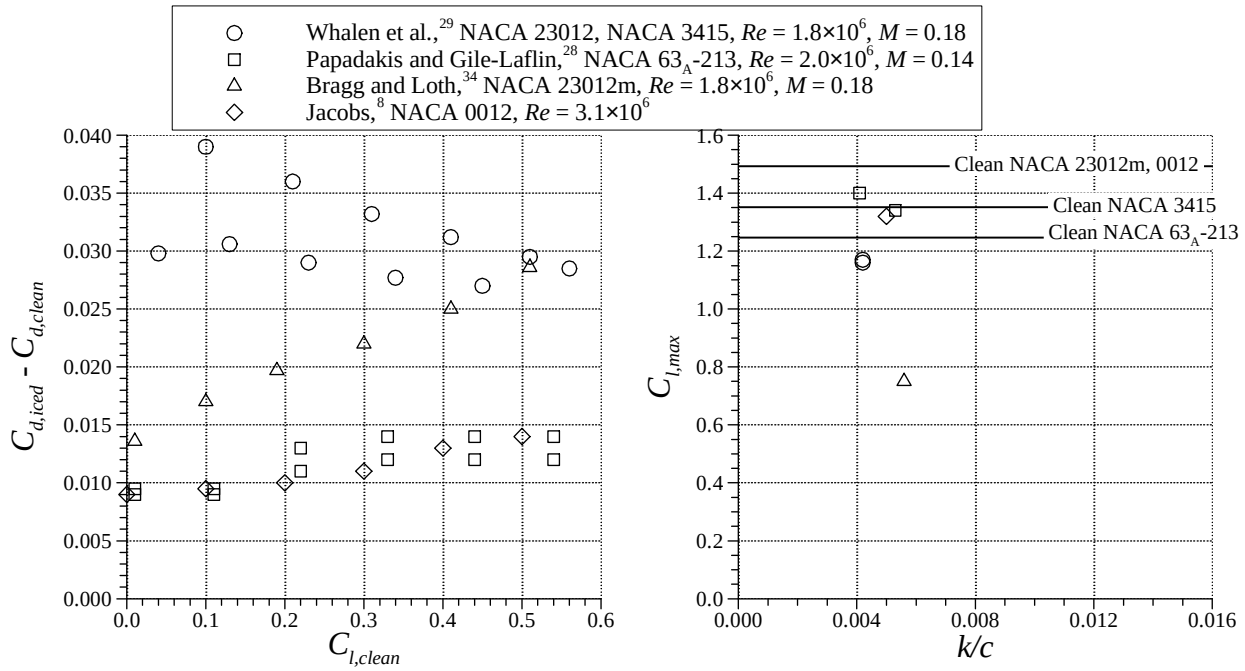

Fig. 15 Effect of various spanwise-ridge shapes on drag (left) and maximum lift. Whalen et al.,[29] data are for simulated runback ridges with *k*/*c* = 0.0035 to 0.005 at x/c = 0.16 on the upper surface and *k*/*c* = 0.008 to 0.014 at *x*/*c* = 0.20 on the lower surface. Papadakis and Gile-Laflin[28] data are for *k*/*c* = 0.0041 triangular and 0.0053 spoiler geometries at *x*/*c* = 0.15 on the upper surface. Bragg and Loth[34] data are for *k*/*c* = 0.0056 quarter-round geometry at *x*/*c* = 0.14 on the upper surface. Jacobs[8] data are for *k*/*c* = 0.005 protuberance at *x*/*c* = 0.15 on the upper surface.

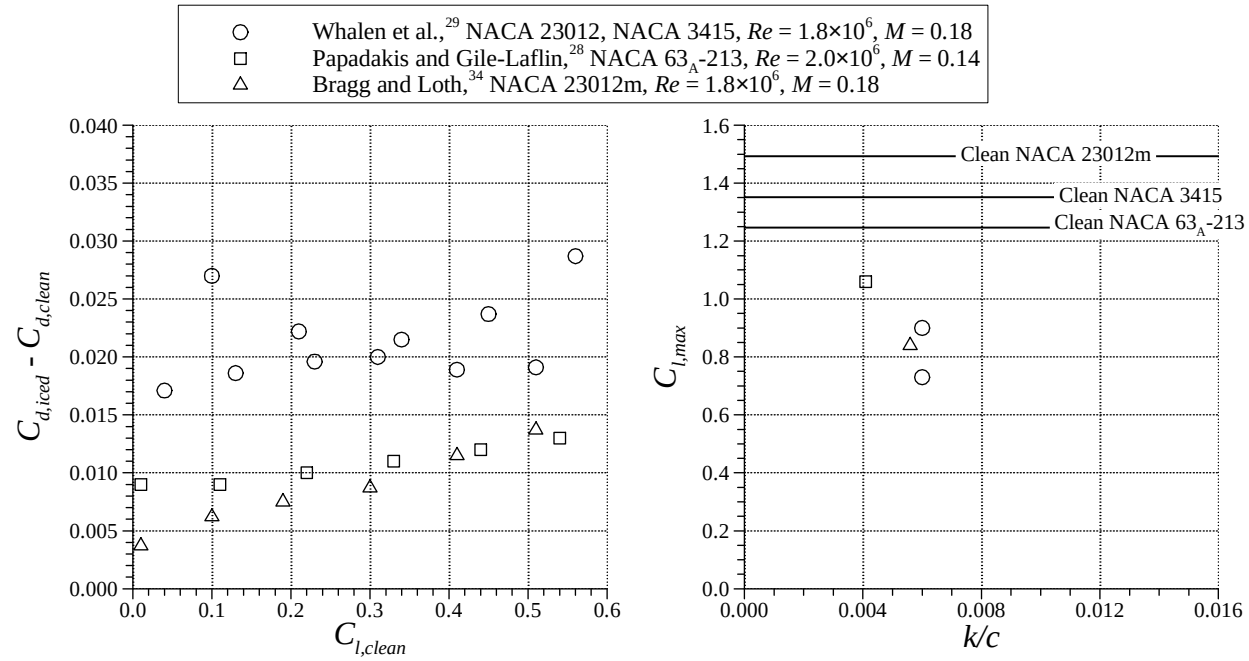

Fig. 16 Effect of various spanwise-ridge shapes on drag (left) and maximum lift. Whalen et al.,[29] data are for simulated runback ridges with *k*/*c* = 0.005 to 0.007 at *x*/*c* = 0.015 on the upper surface and *k*/*c* = 0.006 at *x*/*c* = 0.035 on the lower surface. Papadakis and Gile-Laflin[28] data are for *k*/*c* = 0.0041 triangular geometry at *x*/*c* = 0.025 on the upper surface. Bragg and Loth[34] data are for *k*/*c* = 0.0056 quarter-round geometry at *x*/*c* = 0.02 on the upper surface.

located much closer to the leading edge, they are on the order of ten times larger than the local boundary-layer thickness (cf. Fig. 5). Therefore, the ridge geometry and clean airfoil geometry play less of a role than in the previous case (Fig. 15), where such a large spread in the data was observed.

For the case of SLD-ridge type ice like those shown in Fig. 13, the authors are unaware of any aerodynamic data available for high-fidelity simulations of the ice accretion. Instead, there have been numerous studies that have looked at very simple geometric simulations. While these studies have yielded immensely valuable insight into size and location effects on various airfoils, it is difficult to relate the performance degradations to actual ice accretions. An example of some of these data are shown in Fig. 17. All of the data shown are for a simple geometric upper-surface ridge. For Bragg and Loth,[34] the quarter-round geometry had $k/c = 0.0139$ and was located at $x/c = 0.06$. For Papadakis and Gile-Laflin,[28] the triangular geometry had $k/c = 0.0115$ and was located at $x/c = 0.05$. For Jacobs,[8] the protuberance had $k/c = 0.0125$ and was located at $x/c = 0.05$. These ridge simulations were chosen to correspond to the ridges shown in Figs. 6 and 13, both of which were located at $x/c \approx 0.06$ and had $k/c \approx 0.015$. The lift and drag data in Fig. 17, show a large range of effects. For the NACA 23012 and 0012 airfoils, there is an extremely large increase in drag with C_l. This occurred because the airfoils with the ridges attached stalled at very low C_l — 0.35 for the NACA 23012 and 0.50 for the NACA 0012. For the other two airfoils, the drag rise due to the ridge shape did not increase in the same way because the maximum lift values were higher. The maximum lift value for the casting simulation of the accretion shown in Fig. 6 was 0.78 (cf. Fig. 7). This is over a factor of two larger than the value of 0.35 for the quarter-round geometry in Fig. 17. Based on this, it is not surprising that the associated drag penalty was also much lower. It is likely that the large difference in performance was due, in part, to the spanwise variability of the ridge shown in Fig. 6. It was really made up of a discontinuous row of large ice chunks. Also present in Fig. 6 was ice accretion on the leading edge, upstream of the ridge. The presences of this ice may have reduced the effect of spanwise ridge. Broeren et al.[5] provide a more detailed comparison of these cases with simple geometric ridge simulations.

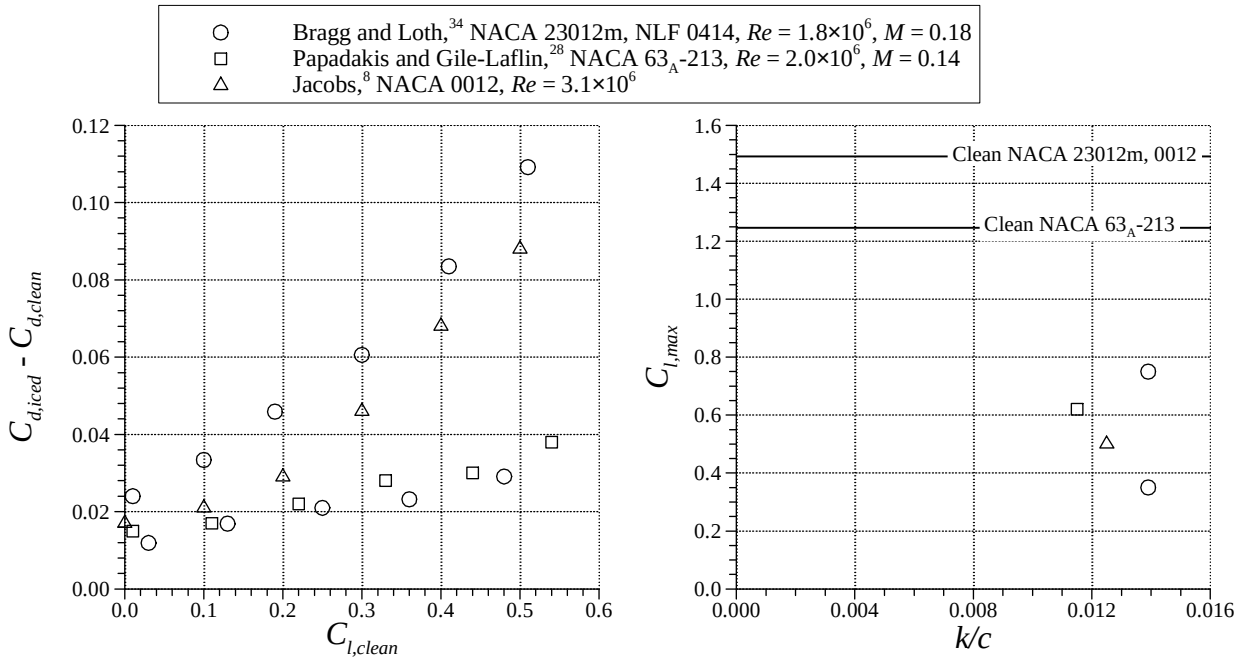

Fig. 17 Effect of various spanwise-ridge shapes on drag (left) and maximum lift. Bragg and Loth[34] data are for $k/c = 0.0139$ quarter-round geometry at $x/c = 0.06$ on the upper surface. Papadakis and Gile-Laflin[28] data are for $k/c = 0.0115$ triangular geometry at $x/c = 0.05$ on the upper surface. Jacobs[8] data are for $k/c = 0.0125$ protuberance at $x/c = 0.05$ on the upper surface.

Figures 14 to 17 illustrate the need for aerodynamic data for iced-airfoil configurations that have high-fidelity spanwise-ridge simulations such as ice castings. Numerous studies have shown that the aerodynamic penalties of ridge-type accretions can be very large for simple geometries.[23,24,26] The question is: how well do these simple geometries actually simulate a real ice accretion? Bragg et al.[3] point out that factors like cross-sectional geometry and spanwise variation can result in large variations in performance degradations. Lee[35] notes that iced $C_{l,max}$ values can be at least a factor of two larger due to changes in geometry and spanwise gaps in a $k/c = 0.0139$ ridge located at $x/c = 0.10$ on the upper surface of a NACA 23012m airfoil. The data presented in Figs. 14 to 17 would certainly support this conclusion. Without high-fidelity aerodynamic data, it is difficult to judge what the true performance degradations are. Bragg et al.,[3] suggest in their review that spanwise-ridge geometries can have potentially the largest aerodynamic effect. This may well be true, but these data indicate that runback ridges may have performance effects on the order of initial roughness. Thus, there is a potential overlap with the previous ice-shape classifications as discussed in connection with intercycle ice. Further study may lead to an expansion of the classification of these ice accretions, or perhaps, to another classification altogether.

IV. Reynolds Number Effects

Nearly all of the aerodynamic data compiled in this paper were in the range of $Re = 1.8\times10^6$ to 3.1×10^6, except for the standard roughness data (Fig. 10) and the measurements made during icing tests. These lower-Reynolds number data were selected in order to facilitate comparison across the various airfoils and icing simulations considered. Fortunately, much is known about Reynolds and Mach number effects on iced airfoils. Bragg et al.,[3] provide a detailed discussion on this, particularly for large ice accretions. For clean airfoils, increases in Reynolds number from 2.0×10^6 to 10×10^6 significantly increase $C_{l,max}$ and reduce the drag. The percentage change in these quantities varies depending upon the type of airfoil. In contrast, iced-airfoil $C_{l,max}$ and drag are relatively insensitive to changes in Reynolds number. This means that nearly all of the conclusions about ice remnants given in this paper should be valid at higher Reynolds number. In fact, aerodynamic data for the intercycle ice accretion simulations on the NACA 23012 was obtained for Reynolds numbers as high as 10.5×10^6.[5,6,19] The minor changes in Reynolds number observed would in no way alter the conclusions of this paper. In addition, Broeren et al.[5,6,19] also provide higher Reynolds number validation for the sandpaper roughness data. In this case, there is slightly more change with Reynolds number, but it is still only a fraction of the clean model Reynolds number dependence. Another roughness study that showed Reynolds number insensitivity to large changes in Reynolds number was due to Morgan et al.[36]

There is one area of ice remnants where Reynolds number considerations may prove to be significant. That is for the spanwise-ridge ice associated with runback ice accretions. The preliminary data shown here indicate that the size of the runback ridges may be on the order of the boundary-layer thickness. In this case, the Reynolds number may play an important role in proper simulation and scaling of the runback ridges between icing-tunnel and aerodynamic testing. Unfortunately, the lack of full-scale data for this case leaves this an open question. In contrast, high Reynolds number testing has been performed for the large, $k/c = 0.0139$ quarter-round ridge shapes on the NACA 23012 airfoil for chordwise locations as far aft as $x/c = 0.20$.[37] In this case, virtually no change in lift and drag performance was observed up to $Re = 10.5\times10^6$. The potential for Reynolds number effects in the case of the runback ridge further suggests that an additional classification of ice shapes may be needed.

V. Conclusion

The overall objective of this paper was to survey previous research on airfoils with ice remnants and summarize what is known about the resulting aerodynamics and performance. It was found that very little aerodynamic data exist for residual ice. The available data indicate a range of drag penalties from those similar to boundary-layer trips to that of uniform, or sandpaper, roughness. However, the maximum lift penalties for residual ice may be much smaller than for uniform roughness. An important difference is that in the case of residual ice, the leading edge may be clear of ice for the first few percent chord, whereas in most roughness studies the roughness is applied around the leading edge. More aerodynamic data are required to understand the flow mechanisms that drive the increase in drag and that may potentially alter the stalling characteristics.

There are a number of good sources of data for intercycle ice accretions where high-fidelity simulations were used for aerodynamic testing. The data indicate that drag increase and maximum lift reduction for intercycle ice accretions resulting from one-minute deicer cycles are similar to those associated with sandpaper roughness. However, when the deicer cycle time was increased to three-minutes large degradations in performance were observed. This implies that the intercycle ice accretions represent an overlap region between roughness and

streamwise ice accretion. It is likely that the boundary-layer separation some of the intercycle shapes was confined to small areas and not a primary driver of the aerodynamics. In other cases, the intercycle ice geometry and performance characteristics were more similar to spanwise-ridge type ice accretion. This means that larger scale areas of separation may be a significant factor in the aerodynamics. Flowfield data, even basic flow visualization, would be very useful to fully document this and better understand how intercycle ice accretion relates to other ice-shape classifications.

Aerodynamic data for high-fidelity simulations of spanwise-ridge ice accretion are scarce. This is unfortunate because the data that do exist represent an enormous range of performance penalties. In some cases, simple geometric simulations of runback ridges were found to result in an increase in maximum lift. While in other cases, large geometric simulations of spanwise (SLD) ridges were found to result in maximum lift coefficients as low as 0.35. It is also known that the cross-sectional and spanwise geometry of spanwise-ridge accretions can be important factors in the aerodynamics. The small size of runback ridges may imply that there are larger Reynolds number effects than have previously been observed for iced airfoils. Because of these factors, it is highly recommended that an effort be undertaken to evaluate the aerodynamics of spanwise-ridge type ice accretions using high-fidelity simulations.

Acknowledgements

The authors were supported in part by NASA and FAA research grants that both directly and indirectly contributed to this work. The support and insight into iced-airfoil aerodynamics from Gene Addy, Mark Potapczuk, Tom Bond, Sam Lee and others at NASA Glenn Research Center along with Jim Riley and Gene Hill at FAA are gratefully acknowledged. The authors also thank Ed Whalen for contributing the boundary-layer thickness data used in this paper.

References

[1] Lynch, F.T., and Khodadoust, A., "Effects of Ice Accretions on Aircraft Aerodynamics," *Progress in Aerospace Sciences*, Vol. 37, 2001, pp. 669-767.

[2] Cebeci, T., and Kafyeke, F., "Aircraft Icing," *Annual Review of Fluid Mechanics*, Vol. 35, 2003, pp. 11-21.

[3] Bragg, M.B., Broeren, A.P., and Blumenthal, L.A., "Iced-Airfoil Aerodynamics," *Progress in Aerospace Sciences*, Vol. 41, No.5, July 2005, pp. 323-362.

[4] Society of Automotive Engineers, S.A.E. Aerospace Information Report, AIR5504, Sept. 2002.

[5] Broeren, A.P., Bragg, M.B., and Addy, H.E. Jr., "Effect of Intercycle Ice Accretion on Airfoil Performance," *Journal of Aircraft*, Vol. 41, No. 1, Jan.-Feb., 2004, pp. 165-174.

[6] Broeren, A.P., and Bragg, M.B., "Effect of Residual and Intercycle Ice Accretions on Airfoil Performance," Dept. of Transportation, Federal Aviation Administration Report DOT/FAA/AR-02/68, May 2002.

[7] Gray, V.H., and von Glahn, U.H., "Effect of Ice and Frost Formations on Drag of a NACA 65_1-212 Airfoil for Various Modes of Thermal Ice Protection," NACA TN-2962, June 1953.

[8] Jacobs, E.N., "Airfoil Section Characteristics as Affected by Protuberances," NACA Rep. 446, 1932.

[9] Bowden, D.T., "Effect of Pneumatic De-Icers and Ice Formations on Aerodynamic Characteristics of an Airfoil," NACA TN-3564, Feb. 1956.

[10] Albright, A.E., Kohlman, D.L., Schweikhard, W.G., and Evanich, P., "Evaluation of a Pneumatic Boot Deicing System on a General Aviation Wing Model," NASA TM-82363, June 1981.

[11] Bond, T.H., Shin, J., Mesander, G.A., "Advanced Ice Protection Systems Test in the NASA Lewis Icing Research Tunnel," NASA TM-103757, May 1991.

[12] Shin, J., and Bond, T.H., "Surface Roughness Due to Residual Ice in the Use of Low Power Deicing Systems," AIAA Paper 93-0031, Jan. 1993, also NASA TM-105971, Jan. 1993.

[13] Bond, T.H., and Shin, J., "Results of Low Power Deicer Tests on a Swept Inlet Component in the NASA Lewis Icing Research Tunnel," AIAA Paper 93-0032, Jan. 1993.

[14] Bond, T.H., Shin, J., Mesander, G.A., and Yeoman, K.E., "Results of the USAF/NASA Low-Power Ice Protection Systems Test in the NASA Lewis Icing Research Tunnel," NASA TP-3319, Sept. 1993.

[15] Reichhold, J.D., and Bragg, M.B., "Residual Ice Characteristics and the Resulting Aerodynamic Performance Penalties," AGATE WP4.010, May 1998.

[16] Jackson, D.G., and Bragg, M.B., "Aerodynamic Performance of an NLF Airfoil with Simulated Ice," AIAA Paper 99-0373, Jan. 1999.

[17] Jackson, D.G., "Effect of Simulated Ice and Residual Ice Roughness on the Performance of a Natural Laminar Flow Airfoil," M.S. Thesis, Dept. of Aeronautical and Astronautical Eng., Univ. of Illinois at Urbana-Champaign, Urbana, Illinois, 1999.
[18] Gile-Laflin, B.E., and Papadakis, M., "Experimental Investigation of Simulated Ice Accretions on a Natural Laminar Flow Airfoil," AIAA Paper 2001-0088, Jan. 2001.
[19] Broeren, A.P., Addy, H.E. Jr., and Bragg, M.B., "Effect of Intercycle Ice Accretions on Airfoil Performance," AIAA Paper 2002-0240, Jan. 2002.
[20] Broeren, A.P., and Bragg, M.B., "Effect of Airfoil Geometry on Performance with Simulated Intercycle Ice Accretions," *Journal of Aircraft*, Vol. 42, No. 1, Jan.-Feb., 2005, pp. 121-130.
[21] Miller, D.R., Addy, H.E., Jr., and Ide, R.F., "A Study of Large Droplet Ice Accretion in the NASA Lewis IRT at Near-Freezing Conditions," AIAA Paper 96-0934, Jan. 1996.
[22] Addy, H.E., Jr., Miller, D.R., and Ide, R.F., "A Study of Large Droplet Ice Accretion in the NASA Lewis IRT at Near-Freezing Conditions; Part 2," NASA TM-107424, Apr. 1997., Prepared for the International Conference on Aircraft Inflight Icing, FAA Springfield, VA., 1996.
[23] Lee, S., and Bragg, M.B., "Effects of Simulated-Spanwise Ice Shapes on Airfoils: Experimental Investigation," AIAA Paper 99-0092, Jan. 1999.
[24] Lee, S., and Bragg, M.B., "Experimental Investigation of Simulated Large-Droplet Ice Shapes on Airfoil Aerodynamics," *Journal of Aircraft*, Vol. 36, No. 5, Sept.-Oct. 1999, pp. 844-850.
[25] Lee, S., Kim, H.S., and Bragg, M.B., "Investigation of Factors that Influence Iced-Airfoil Aerodynamics," AIAA Paper 2000-0099, Jan. 2000.
[26] Lee, S., and Bragg, M.B., "Investigation of Factors Affecting Iced-Airfoil Aerodynamics," *Journal of Aircraft*, Vol. 40, No. 3, May-June, 2003, pp. 499-508.
[27] Calay, R.K., Holdo, A.E., Mayman, P., and Lun, I, "Experimental Simulation of Runback Ice," *Journal of Aircraft*, Vol. 34, No. 2, Mar.-Apr., 1997, pp. 206-212.
[28] Papadakis, M., and Gile-Laflin, B.E., "Aerodynamic Performance of a Tail Section with Simulated Ice Shapes and Roughness," AIAA Paper 2001-0539, Jan. 2001.
[29] Whalen, E.A., Broeren, A.P., Bragg, M.B., and Lee, S., "Characteristics of Runback Ice Accretions and their Aerodynamic Effects," AIAA Paper 2005-1065, Jan. 2005.
[30] Abbott, I.H., and von Doenhoff, A.E., "*Theory of Wing Sections*," Dover Publications, New York, 1959.
[31] Sommers, D.M., "Design and Experimental Results for a Flapped Natural-Laminar-Flow Airfoil for General Aviation Applications," NASA TP-1865, June 1981
[32] McGhee, R.J., Viken, J.K., Pfenniger, W., Beasley, W.D., and Harvey, W.D., "Experimental Results for a Flapped Natural-Laminar-Flow Airfoil with High Lift/Drag Ratio," NASA TM-85788, May 1984.
[33] Whalen, E.A., Broeren, A.P., and Bragg, M.B., "Reynolds Number Considerations for Aerodynamic Testing of Scaled Runback Ice Accretions," AIAA Paper 2006-0260, Jan. 2006.
[34] Bragg, M.B., and Loth, E., "Effects of Large-Droplet Ice Accretion on Airfoil and Wing Aerodynamics and Control," Dept. of Transportation, Federal Aviation Administration Report DOT/FAA/AR-00/14, April. 2000.
[35] Lee, S., "Effects of Super-cooled, Large-droplet Icing on Aerofoil Aerodynamics," Ph.D. Dissertation, Dept. of Aeronautical and Astronautical Eng., Univ. of Illinois, Urbana, IL, 2001.
[36] Morgan, H.L. Jr., Ferris, J.C., and McGhee, R.J., "A Study of High-Lift Airfoils at High Reynolds Numbers in the Langley Low-Turbulence Pressure Tunnel," NASA TM-89125, July 1987.
[37] Broeren, A.P., Lee, S., LaMarre, C.M., and Bragg, M.B., "Effect of Airfoil Geometry on Performance with Simulated Ice Accretions Volume 1: Experimental Investigation," Dept. of Transportation, Federal Aviation Administration Report DOT/FAA/AR-03/64, Aug. 2003.